Controlling the leader-laggard dynamics in delay-synchronized lasers

Cristina M. González, M. C. Torrent, and Jordi García-Ojalvo
Departament de Física i Enginyeria Nuclear, Universitat Politècnica de Catalunya, Colom 11, E-08222 Terrassa, Spain

(Received 17 May 2007; accepted 16 August 2007; published online 26 September 2007)

We study experimentally the collective dynamics of two delay-coupled semiconductor lasers. The lasers are coupled by mutual injection of their emitted light beams, at a distance for which coupling delay times are non-negligible. This system is known to exhibit lag synchronization, with one laser leading and the other one lagging the dynamics. Our setup is designed such that light travels along different paths in the two coupling directions, which allows independent control of the two coupling strengths. A comparison of unidirectional and bidirectional coupling reveals that the leader-laggard roles can be switched by acting upon the coupling architecture of the system. Additionally, numerical simulations show that a more extensive control of the network architecture can also lead to changes in the dynamics of the system. Finally, we discuss the relevance of these results for bidirectional chaotic communications. © *2007 American Institute of Physics*.
[DOI: 10.1063/1.2780131]

The collective dynamics of networks is usually studied under the assumption that coupling between the network elements is instantaneous. However, coupling signals take a finite time to propagate, and this delay time becomes non-negligible when the local dynamics is faster than the coupling mechanism. In that situation, even if the network elements synchronize their dynamics, they do so with a certain (in general nonzero) time lag between each other. This means that, in a given pair of elements, one of them leads the dynamics and the other one lags behind. Here we study experimentally how to control this leader-laggard dynamics by acting upon the coupling profile of two mutually injected semiconductor lasers. Our results show that when the coupling directionality is varied in a controlled way (from unidirectional to bidirectional), the two lasers exchange their leader and laggard roles at a given coupling configuration (partially bidirectional), but the absolute value of the time lag remains unchanged. Additionally, since the leading element in a system of two coupled chaotic oscillators can act as transmitter in a chaotic communication system, we examine whether the controlled role switching reported here can be used as a strategy for bidirectional single-channel information transmission.

I. INTRODUCTION

In networks of dynamical elements,[1] coupling signals take a finite time to travel from one node to another. When this coupling time is comparable to, or longer than, the characteristic time of the network elements, simultaneous synchronization of the dynamics[2] is usually not possible (except in particular network architectures; see, e.g., Refs. 3–5), and lag synchronization[6,7] arises. This effect has led, for instance, to the concept of polychronization in networks of cortical neurons, which has been suggested to have several functional roles.[8]

Under these conditions, it is important to determine which elements are leading the dynamics and which ones are lagging behind. An important factor is whether the links between the elements are directed or not. In the case of two oscillators coupled via a directed link, the element "emitting" the coupling signal is usually the leader (with the exception, again, of certain coupling setups including delayed feedback loops; see, e.g., Refs. 9–11). If the link is undirected, any of the two elements can lead the dynamics depending on the asymmetries between them; if the elements are similar enough, the roles of leader and laggard switch randomly in time.[12]

In this paper, we investigate the dependence of the leader-laggard dynamics on the coupling configuration in two mutually injected semiconductor lasers. We choose semiconductor lasers for our study because they are very sensitive to external perturbations. Optical injection and optical feedback, for instance, produce a rich variety of dynamical phenomena, including chaos.[13,14] In the presence of optical feedback from an external mirror, and for pump currents close to threshold and feedback levels from low to moderate, the laser output exhibits sudden drops in the emitted light at irregular times (with periods on the order of tens of nanoseconds), followed by a gradual recovery. These power dropouts are, in fact, the envelope of much faster optical pulses (on the order of tens of picoseconds),[15] and are thus called low-frequency fluctuations (LFF).

When the output of a semiconductor laser with feedback, operating in the LFF regime, is introduced into a second laser, power dropouts are also induced in the latter, provided the two lasers are similar enough in their physical properties. The dropouts are synchronized between the two lasers and, in general, the emitter laser leads the dynamics (i.e., the dropouts occur earlier)[16,17] with a time lag equal to the coupling time.[18] Interestingly, a similar dynamics is observed in the case of two *bidirectionally* coupled lasers, even in the absence of an external mirror: coupling destabilizes the la-

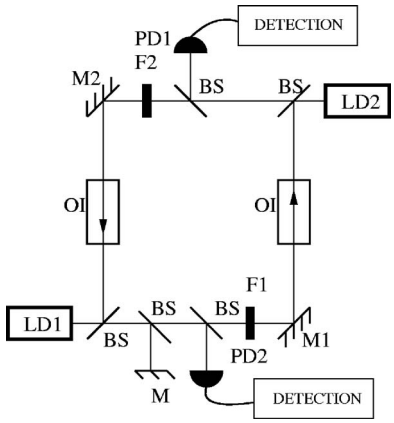

FIG. 1. Experimental arrangement of two semiconductor lasers coupled via two independent unidirectional paths. Laser LD1 receives optical feedback from mirror M. BS, beam splitters; F1 (fixed at 44% transmittivity) and F2 (variable), neutral density filters; M1 and M2, mirrors; OI, optical isolators; PD1 and PD2, photodiodes.

sers and produces a low-frequency dynamics consisting of synchronized dropouts.[12] In that case, however, the leader is determined by the frequency detuning: the laser with higher frequency leads the dynamics, again with a time lag equal to the coupling time. When the two lasers have the same frequencies, the leader and laggard roles alternate randomly between the two lasers. In the bidirectional case, a well defined leader also exists when one of the lasers is subject to feedback;[19] this behavior can again be attributed to the existence of a frequency detuning between the lasers, which in this case is induced by the feedback itself.[20]

In this paper, we examine the transition between the two coupling schemes described above. Specifically, we consider two coupled semiconductor lasers, one of them subject to optical feedback from an external mirror, and vary in a controlled way the directionality of the coupling, ranging from symmetrical bidirectional coupling by common light injection to pure unidirectional injection of the light emitted by the laser with feedback into the other one. As we will see below, this allows us to control which laser leads the dynamics. Numerical simulations also indicate that the dynamical behavior can be qualitatively different between these two coupling setups.

II. EXPERIMENTAL SETUP

Our experimental setup, shown in Fig. 1, consists of two parameter-matched AlGaInP index guided and multiple-quantum-well semiconductor lasers (Sharp GHO6510B2A), coupled by mutual optical injection through two independent unidirectional paths. One of the lasers (LD1) is subject to optical feedback from an external mirror (M). Both lasers operate in a single longitudinal mode with a nominal wavelength of $\lambda_n = 654$ nm. The temperature and pump current of the lasers are controlled with an accuracy of ± 0.01 °C and ± 0.1 mA, respectively, and are adjusted such that the optical frequencies of LD1 (with its feedback) and LD2 (in isolation) are as similar as possible to each other. For temperatures $T_{\mathrm{LD1}} = 21.03$ °C and $T_{\mathrm{LD2}} = 20.34$ °C, the threshold currents of the solitary lasers are, respectively, $I^{\mathrm{th}}_{\mathrm{LD1}} = 31.80$ mA and $I^{\mathrm{th}}_{\mathrm{LD2}} = 32.55$ mA. Optical isolators (Electro-Optics Technology, Inc.), labeled OI in Fig. 1, are placed in the two injection paths in order to have unidirectional coupling in each path. The amount of light injected into each laser is controlled by two neutral density filters (F1 and F2).

The two coupling paths are adjusted such that the coupling times are equal, $\tau_{c1} = \tau_{c2} = 3.4$ ns. The external mirror M that provides feedback to LD1 is also positioned in such way that the feedback time τ_f is equal to the coupling time. The reduction of the threshold current of LD1 due to its feedback is 3.5%. When both lasers are turned on, their threshold currents are also decreased due to the injection. In the absence of the filters F1 and F2 (maximum injection), the threshold reduction of LD1 is 2.6% with respect to its threshold with feedback, and the reduction of LD2 is 2.1% with respect to its free running threshold. The laser outputs are monitored by fast photodetectors of 1 GHz bandwidth (Thorlabs DET210). The received signal is sent simultaneously to a 1 GHz oscilloscope (Agilent DS06104A), and to a spectrum analyzer (Anritsu MS2651B) via two amplifiers (2 GHz bandwidth, Femto high-speed amplifiers). We note that the 1 GHz bandwidth of the detectors smooths out most of the fast pulsing dynamics, resulting in the measurement of only the slower dropout envelopes, which are enough for this study, where the power dropouts are used as low-frequency markers of the dynamics.

III. ALTERNATING THE LEADER AND LAGGARD ROLES IN THE LOW-FREQUENCY FLUCTUATION REGIME

A. Experimental results

In the absence of injection in any of the two coupling paths, laser LD2 is stable while laser LD1 (the one with optical feedback) operates in the LFF regime, and thus undergoes power dropouts at irregular times, as described above. When a sufficient amount of light from LD1 is injected into LD2, this laser exhibits power dropouts as well, following those of LD1 with a natural time lag equal to the coupling time τ_c. This behavior is shown in Fig. 2(a). The time lag can be determined by comparing the times at which synchronized power dropouts occur in the two lasers. A histogram of the time differences between synchronized power dropouts corresponding to this regime is shown in Fig. 2(b). The lag is calculated as the difference between the dropout time in LD1 and the one in LD2, therefore a negative value corresponds to an *advance* of LD1 over LD2, as expected and evident from the vertical dashed lines in Fig. 2(a). Intuitively, this lag is produced by the time needed by the light of one laser to affect the dynamics of the other one. The histogram of time differences has been computed for ~1000 synchronized dropouts. We note that another synchronized state is possible in this setup, in which the lasers are synchronized at zero-lag (provided the feedback and coupling times are equal),[21] but this requires a very careful tuning to make the coupling and feedback strengths equal, and extremely similar lasers;[16] we have not considered that regime here.

We now allow for the light emitted from LD2 to reach LD1 and, varying the transmittivity of filter F2, control the

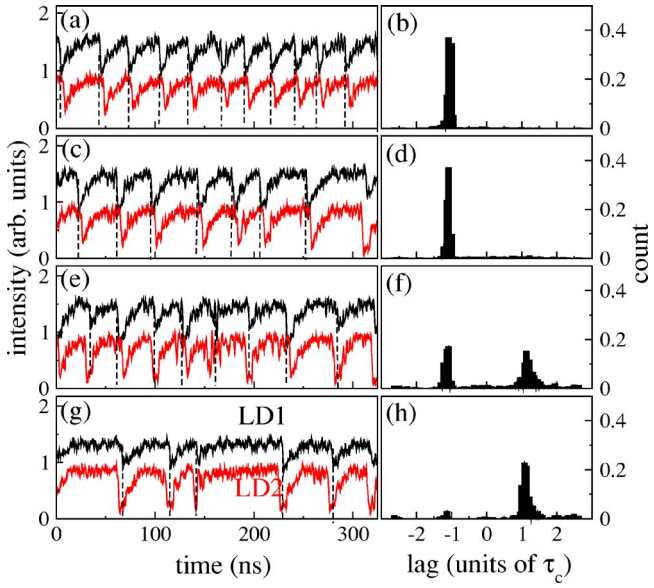

FIG. 2. (Color online) Experimental output intensities (left column) and the corresponding histogram of time differences between synchronized dropouts in the two lasers (right column) for increasing transmittance of the filter F2: (a, b) 0%, (c, d) 40%, (e, f) 63%, (g, h) 100%. The time traces in the left plots have been shifted vertically for clarity, with LD1 corresponding to the top trace and LD2 to the bottom trace in each plot. Vertical dashed lines in those plots signal the occurrence of a dropout in laser LD1.

strength of that coupling while keeping the amount of light injected from LD1 into LD2 constant. Figure 2 shows that for transmittivities up to 40% [Figs. 2(c) and 2(d)] the situation does not change much with respect to the purely unidirectional case (LD1 leads the dynamics a time $\sim\tau_c$), even though a substantial amount of light from LD2 is already entering LD1. At a transmittivity of around 60%, however [Figs. 2(e) and 2(f)], laser LD2 begins to have a certain influence and takes over the leader role sporadically. The situation resembles that of two mutually coupled lasers without mirrors,[12] even though that case is perfectly symmetrical and the present one is not, since one of the lasers (LD1) is subject to feedback and the other one is not. Finally, if we keep increasing the amount of light being coupled back from LD2 into LD1 until the coupling is purely bidirectional [Figs. 2(g) and 2(h)], laser LD2 takes over the leader role permanently, since its dropout precedes almost always those of LD1, again a time $\sim\tau_c$. Throughout this process, the mean period between dropouts increases with coupling strength. The frequency of LD1 decreases with increasing coupling (results not shown), similarly to what happens when feedback levels are increased in the bidirectional configuration.[20] The operating frequency of LD2 matches that of LD1 in the synchronized states (a,b).

B. Numerical simulations

As mentioned above, the dynamical behavior shown in Fig. 2 is the envelope of a much faster underlying dynamics,[15] which cannot be detected by our bandwidth-limited monitoring equipment. In order to determine whether the leader-laggard dynamics described above also holds at these higher frequencies, we resort to numerical simulations of the system. Highly accurate models exist for the dynamics of semiconductor lasers with optical feedback and injection. Our model is based on the Lang-Kobayashi description of a single semiconductor laser with optical feedback,[22] generalized to account for bidirectional coupling,[23]

$$\frac{dE_j}{dt}=\frac{(1+i\alpha)}{2}[G_j-\gamma_j]E_j+\kappa_{c_j}e^{i(\Delta\omega t-\omega_j\tau_{c_j})}E_{3-j}(t-\tau_{c_j})+\delta_{j1}\kappa_f e^{-i\omega_1\tau_f}E_1(t-\tau_f)+\sqrt{2\beta N_j}\xi_j(t), \quad (1)$$

$$\frac{dN_j}{dt}=\frac{I_j}{e}-\gamma_{ej}N_j-G_jP_j(t). \quad (2)$$

The subindex $j=1,2$ denotes lasers LD1 and LD2, respectively, $E_{1,2}$ represents the corresponding optical field, and $N_{1,2}$ is the carrier number. $\omega_{1,2}$ are the free-running optical frequencies of the two lasers, which for simplicity are considered to be the same, so that $\Delta\omega=\omega_2-\omega_1=0$. The optical intensity (or number of photons inside the cavity) is given by $P_{1,2}(t)=|E_{1,2}(t)|^2$. The first term in the right-hand side of Eq. (1) accounts for stimulated emission. The linewidth enhancement factor, α, is assumed to be the same for both lasers, $\gamma_{1,2}$ is the inverse photon lifetime, and $G_{1,2}(t)=g_{1,2}(N_{1,2}-N^0_{1,2})$ is the gain (assumed linear), where $N^0_{1,2}$ denotes the carrier number at transparency and $g_{1,2}$ the differential gain (gain saturation is neglected because the lasers operate close to threshold).

The second term on the right-hand side of Eq. (1) describes the coupling between the lasers, with κ_{c_j} representing the strength of the injection received by laser j and τ_{c_j} being the corresponding coupling time. The coupling strength κ_{c_j} is directly related with the threshold reduction due to injection for each laser. The third term of this equation, which is only present for LD1 (as indicated by the Kronecker delta), is the feedback term, which is described by two parameters: the feedback strength κ_f and the external round-trip time τ_f. The last term of Eq. (1) is the spontaneous emission noise, represented by a Gaussian white noise of zero mean, with spontaneous emission rate β.

The carrier density Eq. (2) is the same for the two lasers. The first term accounts for the pump current $I_{1,2}$, and the second and third terms represent the spontaneous and stimulated recombinations, respectively. We have chosen typical values of the parameters to reproduce the experimental conditions. In particular, the threshold currents are $I^{\text{th}}_{\text{LD1}}=31.80$ mA and $I^{\text{th}}_{\text{LD2}}=32.55$ mA, and the coupling times $\tau_{c_1}=\tau_{c_2}=\tau_f=3.4$ ns. The pump currents are then chosen to be $I_{\text{LD1}}=1.05\times I^{\text{th}}_{\text{LD1}}$ and $I_{\text{LD2}}=1.03\times I^{\text{th}}_{\text{LD2}}$. Other parameters are given in Table I. For this parameter set, the laser with feedback operates in the LFF regime, and we begin with this case in order to compare with the experimental results given above.

Following the experimental process described above, we now introduce different values of κ_{c_1} for constant values of κ_{c_2} and κ_f. Figure 3 shows the output intensities of each laser and the corresponding histograms of the time difference between dropouts for increasing values of the backward coupling rate κ_{c_1}. The numerically computed time series have been filtered with a low-pass fourth-order Butterworth filter

TABLE I. Laser parameters of the numerical model in the LFF regime.

Symbol	Parameter	Value
τ_c	Coupling time	3.4 ns
τ_f	Feedback time	3.4 ns
γ_e	Inverse carrier lifetime	6.89×10^{-4} ns^{-1}
γ	Inverse photon lifetime	0.480 ps^{-1}
N_0	Carrier number at transparency	1.25×10^{8}
g	Gain parameter	1.5×10^{-8} ps^{-1}
α	Linewidth enhancement factor	4.0
β	Spontaneous emission rate	0.5×10^{-9} ps^{-1}
$\omega_1\tau_f$	Phase difference	0.0 rad

with a cutoff frequency of 100 MHz, in order to mimic the limited bandwidth of our experimental equipment. In the case of purely unidirectional coupling, i.e., when no light from LD2 is injected back into LD1 [Figs. 3(a) and 3(b)], LD1 clearly leads the dynamics with a time lag equal to the coupling time τ_c. For increasing coupling from LD2 to LD1 a transition occurs, and at a critical value of that coupling a symmetric situation arises, where the leader and laggard roles alternate randomly in time [Figs. 3(e) and 3(f)]. Note that at the transition point, the total amount of light injected into LD1 (given by $\kappa_{c_1}+\kappa_f=100$ ns^{-1}) is larger than that injected into LD2 ($\kappa_{c_2}=80$ ns^{-1}). Beyond that critical point, LD2 dominates the dynamics. In particular, when the amount of light injected from LD2 to LD1 is higher than in the opposite direction [Figs. 3(g) and 3(h)], LD2 clearly leads the dynamics, again with a time lag equal to the coupling time τ_c. These results are in agreement with the experimental observations shown in Fig. 2.

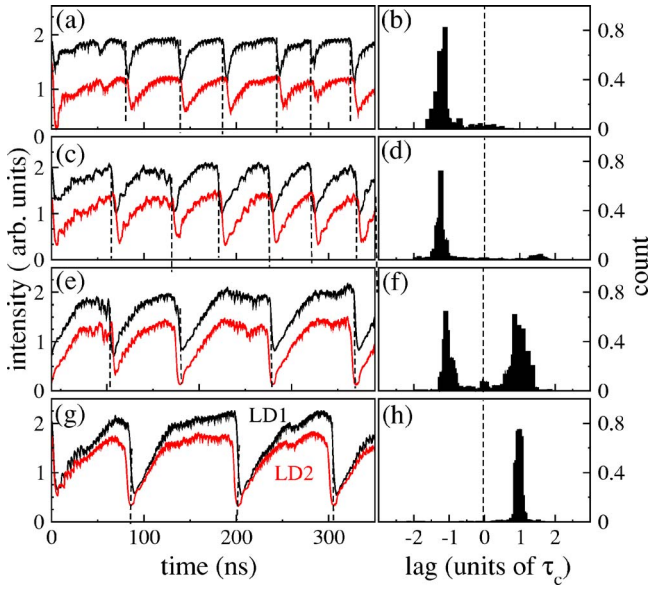

FIG. 3. (Color online) Numerical output intensities (left column) and the corresponding histogram of time differences (right column) for increasing strengths of the injection received by LD1 from LD2, κ_{c_1}. The coupling strength, from LD1 to LD2, is fixed to $\kappa_{c_2}=80$ ns^{-1}, and the feedback strength to $\kappa_f=30$ ns^{-1}. The values of κ_{c_1} are (a, b) 0 ns^{-1}, (c, d) 50 ns^{-1}, (e, f) 70 ns^{-1}, and (g, h) 90 ns^{-1}. Other parameters are given in Table I.

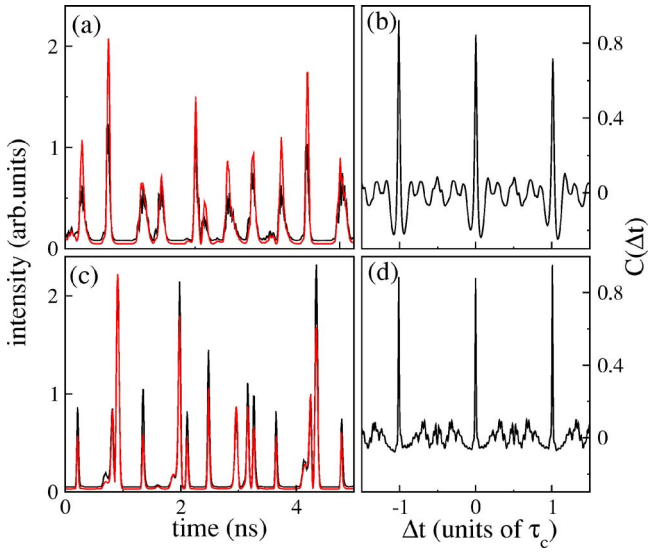

FIG. 4. (Color online) Numerical time series (unfiltered) of the output intensities of the two lasers in the LFF regime (left column) and the corresponding cross-correlation functions (right column). The intensity of one of the lasers has been shifted in time by τ_c to facilitate comparison. The pump currents of the lasers are 1.04 times their threshold values. The coupling parameters are $\kappa_{c_2}=80$ ns^{-1}, $\kappa_f=30$ ns^{-1}, and $\kappa_{c_1}=0$ ns^{-1} (a, b); $\kappa_{c_1}=90$ ns^{-1} (c, d). Other parameters are listed in Table I.

In order to quantify the synchronization level and time lag between the intensity signals for fast time scales (i.e., without filtering), we calculate the cross-correlation function between the two time series,[24]

$$C(\Delta t)=\frac{\langle[P_1(t)-\langle P_1\rangle][P_2(t+\Delta t)-\langle P_2\rangle]\rangle}{\sqrt{\langle[P_1(t)-\langle P_1\rangle]^2\rangle\langle[P_2(t)-\langle P_2\rangle]^2\rangle}}, \tag{3}$$

where the angular brackets denote temporal averages. According to this definition, a maximum correlation at a positive time lag Δt indicates that LD2 is leading the synchronized dynamics with that time lag, and vice versa. Figure 4 represents the unfiltered time series of the lasers, with its corresponding cross-correlation function for two limiting cases. In the unidirectional case [Figs. 4(a) and 4(b)], the fast dynamics is synchronized, and the cross-correlation function shows that laser LD1 leads the dynamics, as expected from the results given above. In the presence of sufficiently large injection from LD2 back into LD1, the leader and laggard roles switch and now LD2 is the leader. This behavior coincides with the dynamics of the signal envelopes (Fig. 2).

Numerical simulations allow us to study with more detail the transition described so far. To that end, we calculated the histograms of intervals between dropouts and the corresponding cross-correlation functions of the unfiltered time series, around the critical value $\kappa_{c_1}=70$ ns^{-1}. The results are plotted in Fig. 5. As shown in that figure, the system passes through a compound state where the dropouts occur both at zero lag and with an alternating leader [Figs. 5(c) and 5(e)]. The corresponding cross-correlation functions of the unfiltered signals (right plots) exhibit a maximum peak at a distance $\pm\tau_c$ for the extreme cases [Figs. 5(b) and 5(h)], while for intermediate values of κ_{c_1} close to the transition [Figs. 5(d) and 5(f)], a maximum peak at zero lag appears. The zero

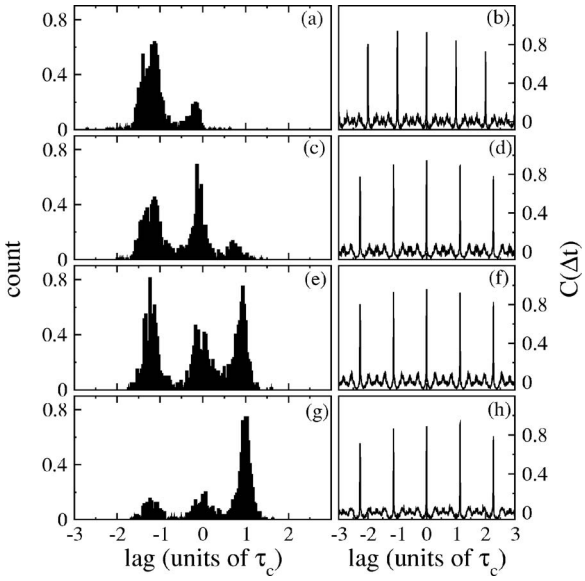

FIG. 5. Histograms of time intervals between power dropouts (left column), and the corresponding cross-correlation functions of unfiltered signals (right column) for increasing strength of the injection received by LD1 from LD2, κ_{c_1}. The coupling strength from LD1 to LD2 is fixed to $\kappa_{c_2}=80$ ns^{-1}, and the feedback strength to $\kappa_f=30$ ns^{-1}. The values of κ_{c_1} are (a, b) 60 ns^{-1}, (c, d) 65 ns^{-1}, (e, f) 70 ns^{-1}, and (g, h) 80 ns^{-1}. Other parameters are given in Table I.

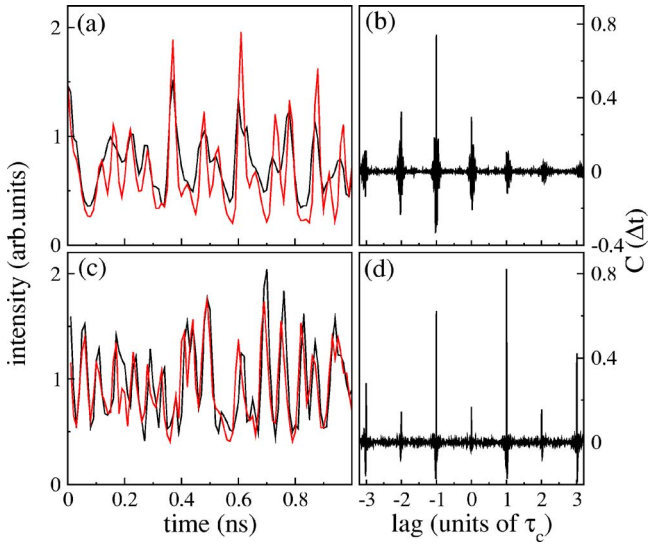

FIG. 6. (Color online) Numerical time series of the output intensities of the lasers in the coherence collapse regime (left column) and the corresponding cross-correlation function (right column). The intensities have been shifted by τ_c to facilitate comparison. The pump currents of the lasers are 1.9 times their threshold values. The coupling parameters are $\kappa_{c_2}=80$ ns^{-1}, $\kappa_f=30$ ns^{-1}, and $\kappa_{c_1}=0$ ns^{-1} (a, b); $\kappa_{c_1}=90$ ns^{-1} (c, d). Other parameters are listed in Table I, except $\alpha=5$, $\beta_1=1.5\times10^{-9}$ ps^{-1}, and $\beta_2=2\times10^{-9}$ ps^{-1}.

lag peak at the intermediate state arises because the feedback and coupling times are equal. When these two times are chosen to be different, the transition occurs via an alternating state where peaks at $\pm\tau_c$ coexist, in the absence of a peak at zero or any other lag time (results not shown). Thus, the phenomenon does not rely on a careful matching of the feedback and coupling times, but is rather most likely due to a shift in the frequency of LD1 when the amount of light injected into it varies (through variation of κ_{c_1}).[20]

IV. OTHER DYNAMICAL REGIMES

We have seen so far that our model reproduces satisfactorily the experimental observations, and shows that the leader-laggard dynamics holds at smaller time scales. We now turn our attention to other dynamical regimes exhibited by this system. When the pump current is higher than the ones considered previously, it is know that the lasers exhibit a fully chaotic dynamics, a regime known as coherence collapse.[25] We have examined whether the leader-laggard dynamics is maintained in that regime, and if the roles can be made to switch by controlling the directionality of the coupling, as in the LFF case. Figure 6 compares the time traces and the corresponding cross-correlation functions in the two limiting cases of unidirectional and bidirectional coupling. The data show that the leader and laggard role are opposite, as in the previous case.

With the aim of determining the boundaries of the dynamical behavior described above, we have also examined numerically, in a systematic way, whether a change in the coupling strength produces a variation in the type of dynamics exhibited by the coupled system. Our results indicate that, without varying other parameters, even under large variations in the coupling from LD2 into LD1, κ_{c_1}, the system does not change its dynamical behavior. Only when the feedback strength κ_f varies the dynamics of the lasers are modified. Figure 7 shows the consequences of varying the feedback strength, when the coupling strengths in the two directions are nonzero. Starting from a synchronized dropout regime, for fixed values of $\kappa_{c_1}=15$ ns^{-1} and $\kappa_{c_2}=25$ ns^{-1}, and for increasing values of the amount of feedback acting upon LD1, the figure shows a substantial change in the dynamics of LD2, while LD1 remains in the LFF regime, without loss of synchronization. Specifically, for large feedback strengths, laser LD2 undergoes power jump-ups synchronized with the dropouts of LD1, which have been recently associated with a mechanism of episodic synchronization.[26]

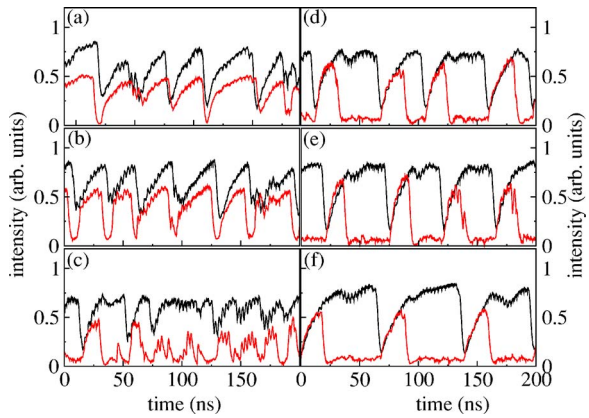

FIG. 7. (Color online) Numerically determined laser output intensities for fixed values of coupling, $\kappa_{c_1}=15$ ns^{-1} and $\kappa_{c_2}=25$ ns^{-1}, and different amounts of feedback on LD1. The time traces of LD1 have been shifted vertically upwards for clarity. (a) $\kappa_f=15$ ns^{-1}, (b) $\kappa_f=20$ ns^{-1}, (c) $\kappa_f=30$ ns^{-1}, (d) $\kappa_f=35$ ns^{-1}, (e) $\kappa_f=40$ ns^{-1}, and (f) $\kappa_f=45$ ns^{-1}.

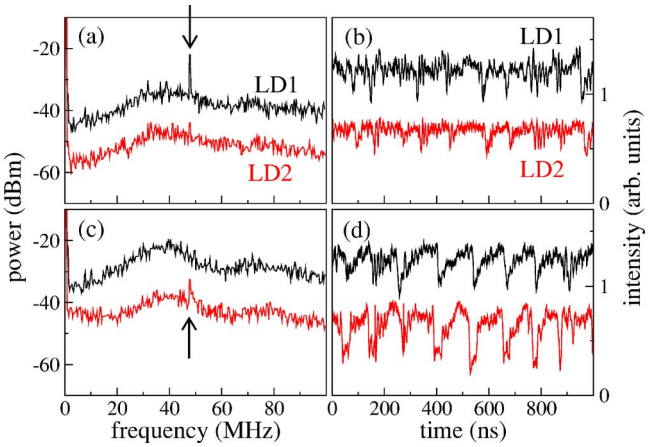

FIG. 8. (Color online) Experimental analysis of the chaos-pass filtering capabilities of the system for unidirectional (a, b) and bidirectional (c, d) coupling. (a, c) RF power spectra, (b, d) corresponding time series. The time traces of LD1 have been shifted vertically for clarity in all plots. The vertical arrows in (a, c) indicate the input modulation in each case. The transmittivity of filter F2 in (c, d) is 63%. Other parameters are those of Sec. II.

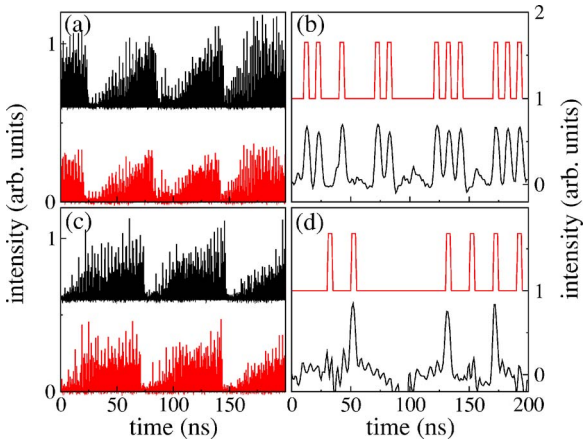

FIG. 9. (Color online) Time traces of emitter and receiver (left) and message extraction (right) in the cases in which (a) the message is introduced in LD1 and recovered by LD2 (LD1 is the leader), and (b) the message in encoded by LD2 and recovered by LD1 (LD2 is the leader). In (a, b) $\kappa_{c_1}=0$ ns^{-1}, in (c, d) $\kappa_{c_1}=90$ ns^{-1}. In the left plots, the upper time trace (shifted vertically for convenience) represents LD1 and the lower time trace corresponds to LD2. In the right plots, the upper trace is the input message and the lower trace is the recovered message. The feedback strength is $\kappa_f=30$ ns^{-1}, other parameters as in Sec. III.

This behavior could in principle be explained by a reduction in the mean frequency of laser LD1 when its feedback level is increased,[20] together with the dynamical behavior of that frequency characteristic of the LFF regime.[26]

V. CONSEQUENCES FOR BIDIRECTIONAL CHAOTIC COMMUNICATIONS

Many studies have examined the viability of message transmission between two coupled chaotic lasers. Most of them have been devoted to unidirectional transmission schemes,[21,27] but the possibility of transmitting information bidirectionally through the same channel is beginning to attract attention. This type of communication obviously requires bidirectional coupling between the lasers, and therefore it is natural to ask whether the relatively simple setup considered in this paper, namely two semiconductor lasers coupled face to face, is useful for bidirectional communications.

Chaotic communications rely on what is known as chaos-pass filtering.[28] Through this mechanism, a message inserted into a chaotic carrier can be decoded by a laser (parameter-matched to the emitter) that filters out the message from the carrier. When synchronization between the lasers occurs with a time lag, as in the case presented in this paper, it is known that only the laggard can act as a chaos-pass filter.[12] This seems to prevent the use of the setup discussed here as a bidirectional communication system. However, we have shown above that we can control which laser leads the dynamics by acting upon the coupling architecture of the system. One could thus envision a protocol that would allow one to switch the leader and laggard roles so that the laser required to act as emitter at any given time leads the dynamics during that time.

First we checked experimentally that switching the leader and laggard roles of the lasers produces also a switching of the chaos-pass filtering characteristics of the lasers. Indeed, as shown in Fig. 8, when a 46-MHz modulation is applied to the pump current of the emitter laser, either LD1 in the case of unidirectional coupling or LD2 in the case of bidirectional coupling (which according to the previous results correspond to LD1 or LD2 leading the dynamics, respectively), the receiver laser filters out the modulation, and no corresponding peak in the radio-frequency spectrum of that laser (the laggard) can be observed. Applying the modulation in the opposite direction, i.e., on the laggard, the modulation peak is maintained in the leader (results not shown).

This is further experimental confirmation of the leader-laggard switch, and hints at the possibility that this system can be used for bidirectional communication by controlling the backward coupling strength κ_{c_1}. We have explored numerically this possibility by introducing a bit message into the pump current of the lasers. Following the situation of Fig. 8, we first transmitted the message from LD1 to LD2, under conditions in which LD1 is the leader, and then transmission was realized from LD2 to LD1, varying the amount of coupling κ_{c_1} in order to make LD2 the leader. The message is decoded by subtracting the light emitted by the two lasers, taking into account the delay between the signals. The bit message is introduced with an amplitude equal to 3% of the pumping current, and the subtracted signal is filtered with a fourth-order Butterworth low-pass filter. Figure 9 compares the two situations of the experiment, and shows that message recovery is better in the unidirectional than in the bidirectional case. The differences in the effectiveness of message recovery indicate that the synchronization quality is not the same in the two regimes considered. Since the cross-correlation function is only an averaged quantity, it does not provide information on potential dynamical deviations from perfect synchronization. In order to quantify such deviations, we computed the sliding correlation coefficient, defined as the maximum of the cross-correlation function, computed

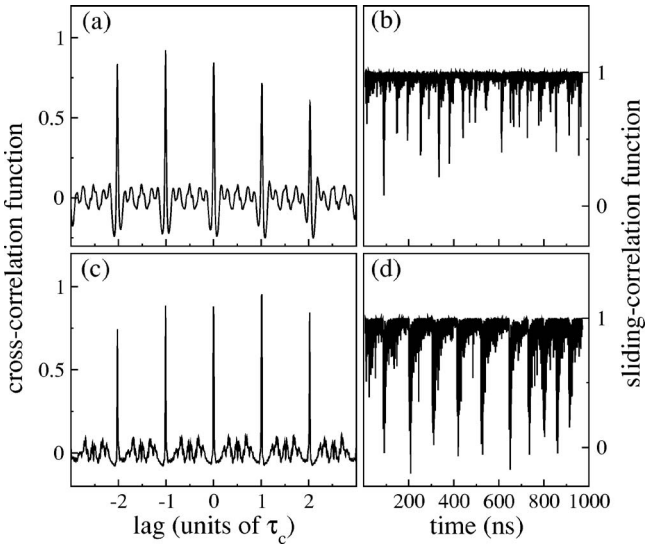

FIG. 10. Cross-correlation (left) and sliding-correlation (right) functions for $\kappa_f=30$ ns^{-1} and different coupling strengths. (a, b) $\kappa_{c_1}=0$ ns^{-1} and $\kappa_{c_2}=80$ ns^{-1}; (c, d) $\kappa_{c_1}=90$ ns^{-1} and $\kappa_{c_2}=80$ ns^{-1}.

with temporal averages over a moving time window of width 3.4 ns.[26] Figure 10 compares this sliding correlation coefficient with the standard cross-correlation function for the two conditions considered in Fig. 9. The figure shows that message recovery is possible in the unidirectional case, even though synchronization is instantaneously lost during the dropouts.[29] In the bidirectional situation, synchronization loss is widespread, which leads to a poor message recovery when the direction of information transmission is from LD2 to LD1. This is the reason why, even though the maximum correlation is similar in both cases [Figs. 10(a) and 10(c)], we cannot recover the message efficiently when transmitting from LD2, even though this laser leads the dynamics.

VI. CONCLUSIONS

We have examined how a system of two coupled chaotic oscillators behaves under conditions of lag synchronization. Our experimental setup consists of two semiconductor lasers coupled via mutual injection of their emitted fields, and allows for the control of the coupling directionality. Our results show that the laser leading the dynamics changes depending on the coupling scenario. When one of the lasers has autonomous chaotic dynamics, in the form of irregularly spaced sudden power dropouts (low-frequency fluctuations), and this dynamics is injected into a solitary laser (which is stable in the absence of injection), the injecting laser obviously leads the dynamics. Such a role, however, can be transferred to the other laser by converting the coupling from unidirectional to bidirectional. The transition occurs via a regime in which the two lasers alternate randomly the leader and laggard roles. This type of behavior is not only restricted to the low-frequency dynamics that we have studied experimentally, but also to fully developed chaotic dynamics (coherence collapse) that occurs for higher pump currents, as shown by numerical simulations. Our model also shows that the type of dynamics can be changed in a continuous way by acting upon the optical feedback strength acting upon the laser with independent dynamics.

The feedback and coupling mechanisms considered in this paper arise from coherent optical injection. It would be of interest to study whether incoherent coupling leads to similar phenomena, since many dynamical systems in nature are coupled incoherently. We can expect that the results would be unchanged in the limiting cases of purely unidirectional and bidirectional coupling, i.e., one or the other dynamical element would lead the dynamics for a time equal to the coupling time. It remains to be seen how the transition between the two regimes would occur in the incoherent case.

Finally, we have discussed the potential of this system for bidirectional chaotic communications. Our experimental results show that whenever one of the lasers leads the dynamics, the other laser (the laggard) is able to operate as a chaos-pass filter. However, we have not been able to send information bidirectionally in an effective way. Numerical simulations show that, even though the maximum cross correlation is similar in both the unidirectional and bidirectional cases, sudden synchronization losses in the latter situation prevent the system from being used as a reliable setup for bidirectional chaotic communications. An alternative scheme has been recently designed that allows for bidirectional transmission of information by sustaining zero-lag synchronization via a dynamical relay.[4,30] Together, these results show the importance of coupling times in delay-coupled dynamical systems.

ACKNOWLEDGMENTS

We thank Javier M. Buldú for useful discussions. This research was supported by the Ministerio de Educacion y Ciencia (Spain) under projects FIS2005-07931-C03-03 and FIS2006-11452, by the Generalitat de Catalunya, and by the GABA project (European Commission, FP6-NEST Contract No. 043309).

[1] S. Boccaletti, V. Latora, Y. Moreno, M. Chavez, and D. U. Hwang, Phys. Rep. **424**, 175 (2006).
[2] S. Boccaletti, J. Kurths, G. Osipov, D. L. Valladares, and C. S. Zhou, Phys. Rep. **366**, 1 (2002).
[3] S. Sivaprakasam, J. Paul, P. S. Spencer, P. Rees, and K. A. Shore, Opt. Lett. **28**, 1397 (2003).
[4] I. Fischer, R. Vicente, J. M. Buldú, M. Peil, C. R. Mirasso, M. C. Torrent and J. García-Ojalvo, Phys. Rev. Lett. **97**, 123902 (2006).
[5] M. W. Lee, J. Paul, C. Masoller, and K. A. Shore, J. Opt. Soc. Am. B **23**, 846 (2006).
[6] M. G. Rosenblum, A. S. Pikovsky, and J. Kurths, Phys. Rev. Lett. **78**, 4193 (1997).
[7] E. M. Shahverdiev, S. Sivaprakasam, and K. A. Shore, Phys. Lett. A **292**, 320 (2002).
[8] E. M. Izhikevich, Neural Comput. **18**, 245 (2006).
[9] H. U. Voss, Phys. Rev. E **61**, 5115 (2000).
[10] C. Masoller, Phys. Rev. Lett. **86**, 2782 (2001).
[11] M. Ciszak, O. Calvo, C. Masoller, C. R. Mirasso, and R. Toral, Phys. Rev. Lett. **90**, 204102 (2003).
[12] T. Heil, I. Fischer, W. Elsäßer, J. Mulet, and C. R. Mirasso, Phys. Rev. Lett. **86**, 795 (2001).
[13] B. Krauskopf, S. Wieczorek, and D. Lenstra, Appl. Phys. Lett. **77**, 1611 (2000).
[14] T. Heil, I. Fischer, and W. Elsäßer, Phys. Rev. A **58**, R2672 (1998).
[15] I. Fischer, G. H. M. van Tartwijk, A. M. G. Levine, W. Elsässer, E. Göbel, and D. Lenstra, Phys. Rev. Lett. **76**, 220 (1996).

[16]A. Locquet, C. Masoller, P. Mégret, and M. Blondel, Opt. Lett. **27**, 31 (2002).
[17]A. Locquet, C. Masoller, and C. R. Mirasso, Phys. Rev. E **65**, 056205 (2002).
[18]We note, however, that if the coupling and feedback strengths are tuned such that the total injection (feedback+coupling) is equal for the two lasers, and if the feedback time is larger than the coupling delay, the emitter laser can anticipate the receiver (Ref. 10). This synchronization state is, nevertheless, much less common and more difficult to reach than the usual lag synchronization state (Refs. 16 and 17) discussed here.
[19]S. Sivaprakasam, E. M. Shahverdiev, P. S. Spencer, and K. A. Shore, Phys. Rev. Lett. **87**, 154101 (2001).
[20]J. F. Martínez Avila, R. Vicente, J. R. Rios Leite, and C. R. Mirasso, Phys. Rev. E **75**, 066202 (2007).
[21]A. Uchida, F. Rogister, J. Garcia-Ojalvo, and R. Roy, Prog. Opt. **48**, 203 (2005).
[22]R. Lang and K. Kobayashi, IEEE J. Quantum Electron. **16**, 347 (1980).
[23]J. Mulet, C. Masoller, and C. R. Mirasso, Phys. Rev. A **65**, 063815 (2002).
[24]J. M. Buldú, M. C. Torrent, and J. García-Ojalvo, IEEE J. Quantum Electron. **41**, 164 (2005).
[25]C. R. Mirasso, in *Fundamental Issues of Nonlinear Laser Dynamics*, edited by B. Krauskopf and D. Lenstra, AIP Conf. Proc. No. 548 (American Institute of Physics, New York, 2000), Chap. 6.
[26]J. M. Buldú, T. Heil, I. Fischer, M. C. Torrent, and J. García-Ojalvo, Phys. Rev. Lett. **96**, 024102 (2006).
[27]A. Argyris, D. Syvridis, L. Larger, V. Annovazzi-Lodi, P. Colet, I. Fischer, J. García-Ojalvo, C. R. Mirasso, L. Pesquera, and K. A. Shore, Nature (London) **437**, 343 (2005).
[28]I. Fischer, Y. Liu and P. Davis, Phys. Rev. A **62**, 011801 (2000).
[29]This is due to the fact that synchronization is not identical, since the coupling and feedback strengths are not tuned to be equal (Ref. 21).
[30]R. Vicente, C. R. Mirasso, and I. Fischer, Opt. Lett. **32**, 403 (2007).